Effects of Polar Group Saturation on Physical Gelation of Amphiphilic Polymer Solutions

Yunqi Li,[†,‡] Tongfei Shi,[†] Lijia An,*[,†] Jooyoung Lee,[‡] Xiaoyong Wang,[‡] and Qingrong Huang*[,‡]

State Key Laboratory of Polymer Physics and Chemistry, Changchun Institute of Applied Chemistry, Chinese Academy of Sciences, Changchun 130022, People's Republic of China, and Department of Food Science, Rutgers University, 65 Dudley Road, New Brunswick, New Jersey 08901

Received: April 15, 2007; In Final Form: July 17, 2007

Monte Carlo simulation on the basis of the comblike coarse grained nonpolar/polar (NP) model has been carried out to study the polar group saturation effect on physical gelation of amphiphilic polymer solutions. The effects of polar group saturation due to hydrogen bonding or ion bridging on the sol−gel phase diagram, microstructure of aggregates, and chain conformation of amphiphilic polymer solutions under four different solvent conditions to either the nonpolar backbone or the polar side chain in amphiphilic polymer chains have been investigated. It is found that an increase of polar group saturation results in a monotonically decreased critical concentration of gelation point, which can be qualitatively supported by the dynamic rheological measurements on pectin aqueous solutions. Furthermore, various solvent conditions to either the backbone or the side chain have significant impact on both chain conformation and microstructure of aggregates. When the solvent is repulsive to the nonpolar backbone but attractive to the polar side chain, the polymer chains are collapsed, and the gelation follows the mechanism of colloidal packing; at the other solvent conditions, the gelation follows the mechanism of random aggregation.

Introduction

Amphiphilic polymers, which include surfactants (emulsifiers) and most biopolymers, contain both hydrophobic and hydrophilic components that have different affinities to water. They have attracted intensive interest in recent years[1−3] because of their unique self-assembling ability of forming abundant morphological patterns. For many charged biopolymers, hydrogen bonding and ion bridging in the presence of multivalent ions always dominate the inter- and intrachain aggregation. The hydrogen bonding is sensitive to temperature[4−6] and polar molecules such as urea,[7] while the ion bridging is sensitive to pH, the ratio between donor and acceptor, and the ionic strength of polymer solutions. Experiments and theoretical calculations encounter enormous difficulties in order to consider all conditions.[8−12] Therefore, intensive research using computer simulations have been carried out to model amphiphilic polymers and to investigate their properties and phase behaviors during the past few years.[13−16]

For amphiphilic polymer solutions, physicochemical factors including pH, ionic strength, multivalent ions, ratio between donor and acceptor, etc. have significant impacts on their physical properties and phase behaviors. If we focus on the specific interaction pairs (e.g., hydrogen bonding and ion bridging) averaged over each polymer chain, these factors can be reduced to affect the polar group saturation in amphiphilic polymer chains. There are two states (either unsaturated or saturated) in total for amphiphilic polymer chains, with the difference in the number of specific interaction pairs. Therefore, a general relationship between physical properties and phase behaviors of amphiphilic polymer solutions under differing pH, type of salt, ionic strength, and polymer composition can be obtained, and an insight into amphiphilic polymer solutions at the interaction pair scale can be achieved. To explore how the polar group saturation affects the physical properties and phase behaviors of amphiphilic polymer solutions, the first step is to set up a suitable model, which is critical for theoretical calculation and simulation.[17] It is well-known that the coarse grain model is an effective way to study the structure−property relationship of polymers.[18] Tries et al. have successfully used coarse grained bond fluctuation Monte Carlo simulation to model polystyrene melts.[19] The comblike hydrophobic/hydrophilic (labeled as "HP") model has been used to model amphiphilic polymers and study the polymer chain conformation distribution.[15,20−22] Alternatively, the hydrophobic/polar (also labeled as "HP") model has been used to model proteins for a long time,[23] while the head/tail (HT) model has been used to describe the properties of small surfactant molecules.[16,24] However, the coarse grain model has one major limitation: when too many details of polymer chains are ignored, this model may not be able to provide a specific description for a given system.[25,26] A clear discussion on the limitation of the coarse grain approach has never been reported. In fact, in the computer simulation treatment on the specific interaction pairs, the coarse grain model has an expression similar to that of the saturation of amphiphilic polymer. It has been reported that the polar group content in amphiphilic polymer has significant effects on the polymer chains' conformation, aggregation, and phase behavior.[27,28] The studies of the effects of the polar group saturation on the physical properties and phase behavior of amphiphilic polymers can significantly improve our understanding of biopolymers because most biopolymers are amphiphilic in nature. Hydrogen bonding, which is a key contributor to the

* To whom correspondence should be addressed. Telephone: +86-431-5262296 (L.A.); (732) 932-7193 (Q.H.). Fax: +86-431-5685653 (L.A.); (732) 932-6776 (Q.H.). E-mail: ljan@ciac.jl.cn (L.A.); qhuang@aesop.rutgers.edu (Q.H.).

† Chinese Academy of Sciences.

‡ Rutgers University.

10.1021/jp072930b CCC: $37.00
Published on Web 10/03/2007

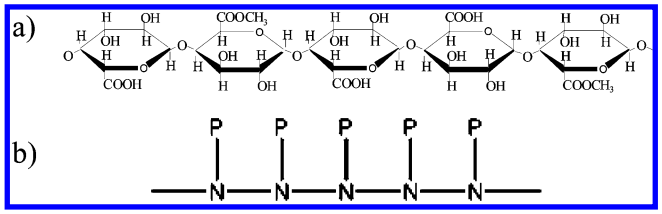

Figure 1. Schematic diagrams of (a) the chemical structure of pectin and (b) the structure of the coarse grained model for amphiphilic polymers with nonpolar backbone (N) and polar side chains (P). The specific interaction pairs among P monomers have strong attractive potential with saturation restriction.

specificity of intramolecular and intermolecular interactions in biological systems,[29] has a saturation feature similar to ion bridging.

On the other hand, pectin, a flexible anionic polysaccharide extracted from plant cells, has been widely used as gelling and thickening agents.[30] The chemical structure of pectin is illustrated in Figure 1a. It is known that, in the presence of Ca^{2+}, pectin with a low degree of methoxyl (DM) content shows remarkably good gelling properties through a cooperative Ca^{2+} ion bridge "egg-box" binding mechanism with the carboxyl group in pectin chain.[31] In the absence of Ca^{2+}, other nonspecific interactions with the carboxyl group in a pectin chain, such as van der Waals force and hydrogen bonding, dominate the aggregation behavior of pectin chains.[32] Since Ca^{2+}-induced chain association severely depends on the content of carboxyl group in a pectin chain, as well as the concentration of either Ca^{2+} or pectin, the changes of these three parameters can be modeled as the polar group saturation of pectin chains. Therefore, pectin aqueous solutions provide a suitable model system to test the simulation results obtained from the investigation of the effects of polar group saturation on physical gelation of amphiphilic polymer solutions.

In this paper, we first present a coarse grain model for amphiphilic polymer solutions and then study the effects of polar group saturation on physical gelation of polymer solutions using a newly improved eight-site bond fluctuation Monte Carlo simulation.[33] Subsequently, dynamic rheological measurements on pectin aqueous solutions are used to test the simulation results. For the comblike coarse grained chain model of amphiphilic polymers, the effects arising from the variation of solvent conditions to the backbone and the side chain on polymer chain conformation and gelation will also be thoroughly discussed.

Monte Carlo Simulation

Monte Carlo simulation is performed in a lattice on the basis of the eight-site bond fluctuation algorithm,[33,34] where polymer chains under thermodynamic equilibrium are generated in a cubic lattice with periodic boundary conditions in all directions. The bond fluctuation algorithm[35] has been proved to be successful in the simulation of comblike polymer systems.[36,37] The number of polymer chains n_P equals $V\phi/2N\upsilon$, and the rest of the sites are filled with solvent molecules of the same size as one monomer in polymer chain, where $V \equiv 128^3$ is the total number of sites in the lattice, $\upsilon \equiv 8$ is the number of lattice sites occupied by each monomer, ϕ is the polymer concentration, and N, fixed at 200 in this work, is the number of monomers in the backbone or side chain in each comblike coarse grained polymer chain with nonpolar backbone (N) and polar side chain (P), i.e., 200 (N−g−P) repeat units in each chain, as illustrated in Figure 1b. For the interactions in the simulation, the interaction among polar groups (ϵ_{PP}) is fixed at $-0.5k_BT$ to hold strong interaction pairs among P monomers. Besides the strong attractive interaction among polar groups, considering different solvent conditions for the backbone and the side chain in the coarse grained comblike chain model,[38,39] four different solvent conditions are considered: case A, in which the solvent molecules have no interactions with either the backbone or the side chain; case B, in which the solvent molecules are attractive to the backbone but have no interactions with the side chain; case C, in which the solvent molecules are attractive to the backbone but repulsive to the side chain; case D, in which the solvent molecules are repulsive to the backbone but attractive to the side chain. The corresponding interactions involved in each solvent condition are listed in Table 1. Here the cutoff of the interaction pair is $\sqrt{6}$.[40] The intrachain aggregation is formed through the chemical bond connection, while the interchain aggregation is formed through the strong attractive interaction pairs among the polar side chain monomers (P). The thermodynamic relaxation motion was implemented through a combination of bond fluctuation[41] and solvent diffusion[42] under the constraint of the Metropolis sampling rule.[43] Twenty-five parallel samples were simulated at each point to obtain accurate results and determine the sol−gel phase diagram. The simulation was carried out using the following steps: (i) polymer chain and solvent molecules were evenly dispersed in the simulation lattice; (ii) the simulation lattices were relaxed without any interactions for 3×10^5 Monte Carlo steps (MCS), with each MCS denoting the simulation time for all the monomers in polymer chains to have one attempt for motion; (iii) all the interactions were "switched on" under different solvent conditions (i.e., cases A, B, C, and D) for an additional 1×10^6 MCS to achieve thermodynamic equilibrium. The criteria to determine whether the system is in the thermodynamic equilibrium state are based on the method described in our previous work.[33]

TABLE 1: Interaction Parameters and Cases of Four Different Solvent Conditions Used in the Monte Carlo Simulation[a]

Cases	ϵ_{PP}	ϵ_{NS}	ϵ_{PS}	R_g/R_{g0}		conformation
				$\phi \to 0$	$\phi = 0.15$	
A	-0.5	0	0	0.85	0.73	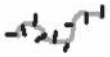
B	-0.5	-0.1	0	0.87	0.76	
C	-0.5	-0.1	0.1	0.94	0.85	
D	-0.5	0.1	-0.1	0.80	0.69	

[a] The interaction is in the unit of k_BT, with k_B and T as the Boltzmann constant and absolute temperature, respectively. All the other interactions that are not included in this table are null. In the schematic diagram of unperturbed single chain conformation in solution, gray lines and black lines represent the nonpolar backbone and polar side chain, respectively. Snapshots of chain conformation picked up from the final simulation configurations ($k_{sa} = 0.36$, $\phi = 0.15$) under different solvent conditions are provided in the Supporting Information (see Figure S2).

The root-mean-square radius of gyration of the amphiphilic polymer chain R_g was calculated using the following equation:

$$R_g = \left\langle \frac{1}{2N} \sum_{i=1}^{2N} (\vec{r}_i - \vec{r}_{cm})^2 \right\rangle^{1/2} \quad (1)$$

where $\vec{r}_i$ is the position of the ith monomer in either the backbone or the side chain and $\vec{r}_{cm}$ is the center of mass of the comblike polymer chain. The $\langle\ \rangle$ represents the ensemble average of all polymer chains over 25 parallel samples at each point.

The diffusion coefficient D_c of a polymer chain is calculated through

$$D_c = \frac{\langle |r_{cm}(t) - r_{cm}(0)|^2 \rangle}{6t} \quad (2)$$

where $r_{cm}(t)$ is the position of the center of mass of a chain at time t, and t is the simulation time in the unit of MCS. The numerator in this equation is the mean-square displacement of the center of mass of polymer chains. The MCS-dependent root-mean-square gyration radius (R_g) and diffusion coefficient (D_c) are provided in the Supporting Information, as shown in Figure S1.

To record the polar group saturation in amphiphilic polymer chains, a parameter k_{sa}, defined as z_{max}/z, is introduced, where z_{max} is the maximum of the specific interaction pairs restriction exerted on each polar group, and z, which equals 14, is the effective coordination number of the lattice model.[34] Since the comblike chain model has taken into account the advantages of both HP and HT models,[15,16,20−24] the saturation of polar group can be comprehended twofold: one is the coarse grain, where k_{sa} represents the ratio between the number of coarse grained units and their corresponding repeat residues in a real polymer; the other is the saturation restriction, where k_{sa} represents the ratio between the maximum number of specific interaction pairs with and without the polar group saturation restriction in each polar group. In this paper, we only consider k_{sa} as the polar group saturation restriction. The physical meaning of k_{sa} is as follows: when $k_{sa} = 0$, the polar group saturation restriction is so strong that all the polar groups (P's) in the amphiphilic polymer chain lose the ability to form strong attractive interaction pairs with other P monomers. No specific interaction pairs exist among polar groups, and no junction can induce interchain aggregation. When $k_{sa} = 1$, any polar group (P) locating in the neighboring sites around another P monomer can form a specific interaction pair. For pectin aqueous solutions, $k_{sa} = 0$ corresponds to the absence of Ca^{2+} in solution, while $k_{sa} = 1$ corresponds to the case when Ca^{2+} is sufficient or excessive to form ion bridges with the carboxyl group in pectin chains.[44] Also, to avoid double bonding or even triple bonding among P monomers, when $k_{sa} > 1/z_{max}$, further coupling between two monomers is prohibited once there is one bond between them.

To have a better understanding of the effects of solvent conditions on the conformation of polymer chain, the expansion factor R_g/R_{g0} was calculated from (1) the solution with the volume fraction fixed at 0.15 ($\phi = 0.15$), and (2) extra simulations for the single chain system ($\phi \to 0$), with 25 parallel samples under each solvent condition after 1×10^6 MCS. R_{g0}, which equals 52.04, is the root-mean-square radius of gyration for the single chain system without any interactions (unperturbed polymer chain). In all the simulations, k_{sa} was fixed at 0.36. The values of R_g/R_{g0} for polymer solutions corresponding to different solvent conditions are listed in Table 1.

Experimental Section

Materials. Pectins of different methoxyl contents were provided by Danisco A/S (Denmark) and purified by dialysis (Spectra/Por dialysis membrane with molecular weight cutoff equal to 12 000) in Milli-Q water, followed by freeze-drying. The average molecular weights (M_n's) of purified pectins were determined by gel permeation chromatography. Table 2 shows the characteristic parameters of the pectin samples used in the experiments. Analytical-grade $CaCl_2$ was purchased from Aldrich Chemical Co. (Milwaukee, WI). Milli-Q water was used in all experiments.

TABLE 2: Characteristic Parameters of the Pectin Samples Used in the Rheological Experiments[a]

badge	M_n (g/mol)	M_{mono} (g/mol)	N	D	DM (%)	DA (%)
P1	607 109	190.5	3187	1.2	32	0
P2	716 247	192.7	3717	1.1	48	0
P3	812 555	190	4277	1.1	31	19

[a] The number-average molecular weights are obtained from gel permeation chromatography. N and D are the degree of polymerization and the dispersion coefficient, respectively. DM and DA, which refer to the degree of methoxyl and amide content, respectively, were provided by Danisco A/S.

Rheological Measurements. The dynamic rheological measurements of different pectin solutions were carried out using a strain-controlled advanced rheometric expansion system (ARES) (TA Instruments, New Castle, DE). The pectin solutions were loaded into Peltier temperature-controlled parallel plates of 50 mm diameter for at least 15 min to allow the stresses to relax and the samples to reach thermal equilibrium at room temperature. A solvent trap device containing wet cotton was used to prevent solvent evaporation from the sample edge. Dynamic frequency sweep experiments were performed in the frequency range from 0.1 to 100 rad/s. Previously, strain sweep tests were carried out to determine the proper conditions of rheological measurements.

Results and Discussion

Monte Carlo Simulation. The sol−gel phase diagram was determined using the method described in our previous work[45] through the treatments of percolation probability. The percolation probability $P(\phi,k_{sa})$, which denotes the probability of a system to be a gel under a given composition and polar group saturation, equals the percentage of percolated samples in all 25 parallel samples at each point. Here the gelation is regarded as a percolation process through a combination of bond percolation along the backbone chain and site percolation through the strong association of P monomers in a side chain. Figure 2 shows the dependence of $P(\phi,k_{sa})$ on polymer concentration with different polar group saturations of amphiphilic polymers under the four different solvent conditions (cases A−D) listed in Table 1. It can be seen that, under each solvent condition, the variation of sol−gel transition with concentration becomes sharper as the polar group saturation increases. For a given polar group saturation, all the simulation results can be well fitted by the sigmoidal Boltzmann equation,[45] which can be described as

$$P(T^*,\phi) = P(T^*,\phi_{UC})\left\{1 + \frac{P(T^*,\phi_{LC}) - P(T^*,\phi_{UC})}{P(T^*,\phi_{UC})}\left[1 + \frac{\exp(\phi - \phi_{LC})}{\Delta\phi}\right]^{-1}\right\} \quad (3)$$

Here, $\Delta\phi$ is the constant interval of ϕ, ϕ_{LC} is the lower critical gelation point, which is generally called the gel point, and ϕ_{UC} is the upper critical gelation point. The lower and upper critical points in the sol−gel transition curves can be obtained from the fitting to eq 3, and the results are plotted in Figure 3.

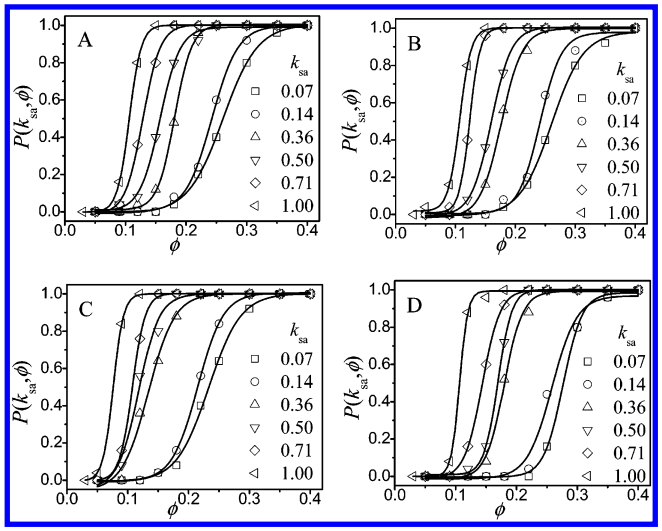

Figure 2. Percolation probability versus polymer concentration at different polar group saturations under four different solvent conditions: case A, case B, case C, and case D described in Table 1. The solid lines are obtained from the sigmoidal Boltzmann fits (eq 3).

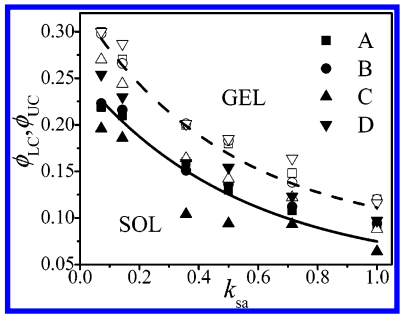

Figure 3. Plot of sol−gel phase diagram constructed under different polymer concentrations, polar group saturations, and solvent conditions. Solid and dashed lines are the fittings to the average of the lower and the upper critical points on the four systems with various solvent conditions.

According to the physical meaning of $P(\phi,k_{sa})$, a simulation sample is a sol when $P(\phi,k_{sa}) = 0$ and a gel when $P(\phi,k_{sa}) = 1$. The sol−gel phase diagram (Figure 3) clearly shows that, when the polar group saturation increases, both the critical concentrations and the concentration region for sol−gel transition monotonically decrease. The shift of the gel point (i.e., the lower critical point in the sol−gel transition) to a lower concentration with the increase of polar group saturation can be related to the Ca^{2+}-induced chain association and gelation in pectin aqueous solutions, where the increase of either the content of carboxyl group or $[Ca^{2+}]$ leads to a lower concentration of gelation and higher storage modulus of the gel.[44,46,47] Furthermore, if we correlate the polar group saturation with the cross-linking probability of P monomers, the increase of polar group saturation corresponds to the increase of cross-linking probability, and our simulation results are consistent with the simulation results by Liu et al.[48,49]

From Figure 3, the effects of solvent conditions on the sol−gel phase diagram of the amphiphilic polymer solution can be described as follows: in case A, both ϵ_{NS} and ϵ_{PS} are zero, and the solvent molecules are nonselective and have no interactions with either polymer backbones or polymer side chains; in case B, ϵ_{NS} is negative, i.e., the solvent molecules are attractive to the backbone, while ϵ_{PS} is zero, and the solvent molecules have no interaction with the side chains. There is a minor difference between case A and case B. In case C, the solvent molecules are attractive to the backbone ($\epsilon_{NS} < 0$) but repulsive to the side chains ($\epsilon_{PS} > 0$); the gelation occurs in diluter solution. In case D, the solvent molecules are repulsive to the backbone ($\epsilon_{NS} > 0$) but attractive to the side chains ($\epsilon_{PS} < 0$); the gelation takes place in concentrated solutions. To make clear how the solvent conditions and polar group saturation affect the physical gelation in amphiphilic polymer solutions, the analyses of micelle clusters and polymer chain conformation are carried out.

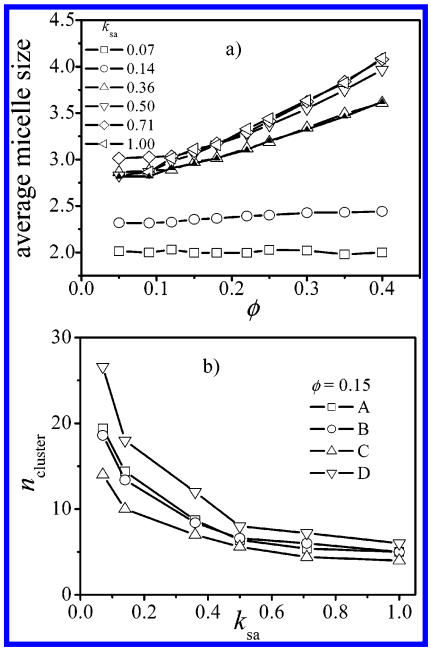

Figure 4. (a) Micelle size dependence on polymer concentration at different polar group saturations. All the data come from case C except for the solid triangles, which are obtained from case D, with $k_{sa} = 0.36$. (b) Dependence of the number of micelle clusters on polar group saturation at different polymer concentrations under four different solvent conditions.

Since in the sol−gel transition not all polymer chains participate in the building of gel network, especially when the system is close to the gel point, the micelles and micelle clusters formed by intra- and interchain association may have broad size distributions.[45] The micelles are formed by the packing of P monomers that are held together through the strong attractive interaction ϵ_{PP}. The micelles can be further bridged by the backbone chain to form micelle clusters. The average micelle sizes, obtained from counting P monomers in each micelle within all the parallel samples followed by a statistical average treatment described in our previous work,[45] are plotted against concentration at different solvent conditions, as shown in Figure 4a. It can be seen that, when k_{sa} is not larger than 0.14 (i.e., two P−P interaction pairs on each P monomer at most), the average micelle size is independent of the polymer concentration because the polar group is easy to become saturated and a larger number of P monomers do not increase the size of micelle; when k_{sa} is larger than 0.14 (i.e., two P−P interaction pairs on each P monomer at least), the average micelle size increases as the polymer concentration increases because the polymer chains need more P monomers to become saturated. When k_{sa} is fixed at 0.36, in case C and case D, the average micelle sizes have almost the same values, suggesting that the solvent conditions have a negligible effect on the micelle sizes. The reason is that the collective long-range nature of solvent conditions has a negligible effect on the micelle formation arising from short-range local monomer association. For the number of micelle clusters $n_{cluster}$, their relationship with polar group saturation is similar at different polymer concentrations, but is quite different at different solvent conditions, as shown in Figure 4b. When

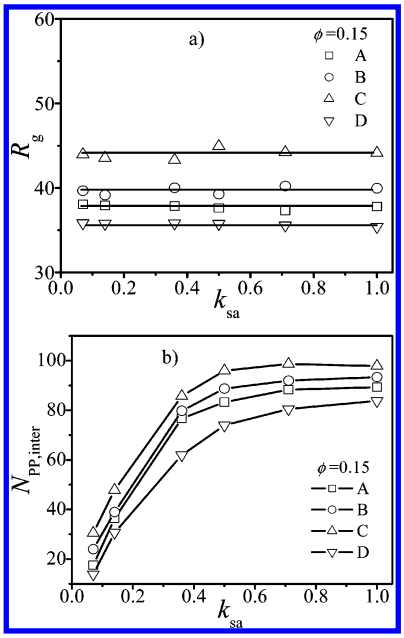

Figure 5. (a) k_{sa} dependence of the root-mean-square radius of gyration under four different solvent conditions. (b) Plot of the number of interchain P−P interaction pairs per chain ($N_{pp,inter}$) versus k_{sa} with polymer concentration fixed at 0.15.

the polar group saturation increases, $n_{cluster}$ monotonically decreases, suggesting that the higher polar group saturation results in a larger micelle cluster. This is reasonable because the sizes of aggregates of P monomers (i.e., micelles) become larger with higher polar group saturation. For the four different solvent conditions, when the solvent molecules become more attractive to the polymer backbone, i.e., from case D to case C, $n_{cluster}$ decreases. This result indicates that the micelle clusters are larger in case C, corresponding to the lower concentration of the gel point in Figure 3, which is coincident with our previous simulation results from other systems, where the gelation occurs in lower concentration solutions when the micelle sizes are large.[50]

As illustrated in Table 1, different solvent conditions can greatly affect chain conformation, resulting in a difference in the number of micelle clusters. Corresponding to the schematic pictures, the typical chain conformations under different solvent conditions are provided in the Supporting Information, as shown in Figure S2, which are snapshots from the configurations under thermodynamic equilibrium state with the volume fraction fixed at 0.15. To study the effects of saturation and solvent conditions on polymer chain conformation, the root-mean-square radius of gyration of the amphiphilic polymer chain R_g was calculated using eq 1, and the results are presented in Figure 5a, which shows that R_g is independent of polar group saturation because it only affects the association of side-chain monomers in the short range, and therefore has a minor effect on chain conformation. It should be emphasized that the sizes of polymer chains in case C are much larger than those in case D, consistent with the sol−gel phase diagram and the effects of the number of micelle clusters. The polymer chains in case C are much more extended than those in case D, and the extended chains are prone to interchain aggregation, leading to the formation of larger micelle clusters (fewer micelle clusters at the same concentration) and lower concentration of the gel point. To provide a direct illustration of why the interchain aggregation in case C is more significant than that in case D, the number of specific P−P interaction pairs among different chains averaged over each chain, $N_{PP,inter}$ was calculated. The polar group saturation dependences of $N_{PP,inter}$ under different solvent conditions are shown in Figure 5b. Within the polar group saturation range studied, $N_{PP,inter}$ in system C is always larger than that in system D, consistent with the polymer chain conformation results discussed above. Similarly, in cases B and C, the solvent molecules are attractive to both polymer backbones; the difference is that the solvent molecules have no interactions with polymer side chains in case B, but have repulsive interaction with polymer side chains in case C. From the comparison between polymer conformation in case C and in case B, our results suggest that the solvent molecules repulsive to the polymer side chain can promote interchain aggregation, leading to a more extended chain conformation in case C than in case B.

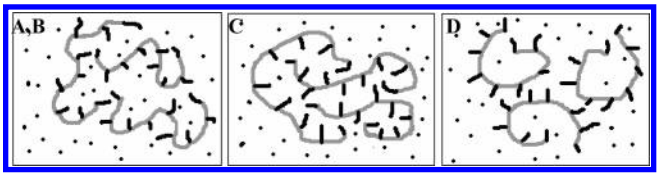

Figure 6. Schematic diagrams of the effects of solvent conditions on the chain conformation and aggregation. The black lines, gray lines, and black points represent the polymer side chain P, backbone N, and solvent, respectively.

In summary, to clearly state how the solvent conditions affect the polymer chain conformation, aggregation, and gelation, the microstructures of the amphiphilic polymer solutions at the single chain scale are illustrated in Figure 6. Here the volume fraction of the polymer chains is fixed at 0.15. The schematic diagrams are described as follows: when solvent molecules are attractive to the polymer backbone but repulsive to the polymer side chain (case C), the sol−gel transition occurs in solutions with a lower polymer concentration. The polymer chains are more extended as indicated by the larger R_g/R_{g0} value (i.e., 0.85), and the micelle clusters are larger. The interchain aggregation occurs on a larger scale, and the gelation follows the mechanism of random aggregation.[51,52] When the solvent molecules are repulsive to the backbone but attractive to the side chain (case D), the sol−gel transition occurs at solutions with higher polymer concentration, the micelle clusters are smaller, and polymer chains are collapsed, as evidenced by the smaller R_g/R_{g0} value (i.e., 0.69). The interchain aggregation occurs on a smaller scale, while the gelation follows the mechanism of colloidal packing.[53,54] When the solvent molecules are nonselective without any interactions with the polymer chain (case A), or are a little attractive to the backbone but noninteractive with the side chain (case B), sol−gel transition occurs in solutions with medium polymer concentration; both micelle clusters and polymer chains are medium in size. The interchain aggregation occurs in random ways, and the gelation follows the mechanism of random aggregation.

Dynamic Rheological Measurements. As discussed previously, the sol−gel phase diagram obtained from Monte Carlo simulation may be applied to the gelation of pectin aqueous solutions. To compare the physical gelation of pectin aqueous solutions with the amphiphilic polymer solutions in Monte Carlo simulation, a series of dynamic rheological measurements on pectin solutions have been carried out. The effects of carboxyl group content, concentration of pectin solution, and [Ca^{2+}] at room temperature on the rheological properties of pectin aqueous solutions have been studied using dynamic rheological measurements, and the results are shown in Figure 7. It is found that for all pectin solutions, in the low-frequency region, both the storage modulus G' and the loss modulus G'' follow the power laws of $G' \sim \omega^{\Delta'}$ and $G'' \sim \omega^{\Delta''}$, where ω is the angular

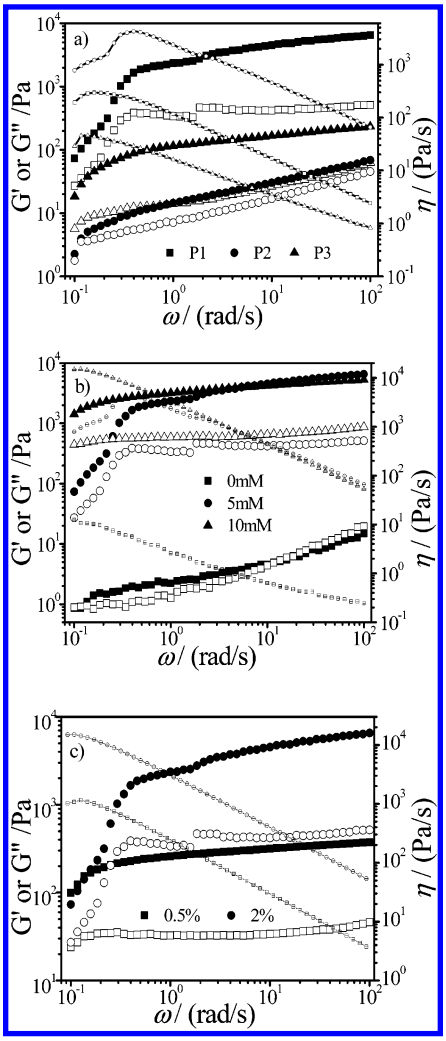

Figure 7. Storage module G' (large solid symbols), loss module G'' (large open symbols), and viscosity η (small symbols) changing with frequency for pectin aqueous solutions at a fixed temperature of 25 °C for (a) different types of pectin, (b) $[Ca^{2+}]$, and (c) pectin concentration.

frequency in rheological measurements. The scaling exponent Δ' is always larger than Δ'', indicating that all the systems exhibit a sol on a long time scale.[55−57] However, at the higher frequency region, both G' and G'' have the same scaling exponent ($\Delta' = \Delta'' = \Delta$), indicating that all the systems are gels on a short time scale.[58] The scaling exponents of different pectin solutions in the high-frequency region, Δ, which presents the degree of perfection of the gel network or the homogeneity of the sample, are listed in Table 3.

Besides these common features, Figure 7a also shows that the storage modulus, the loss modulus, and the viscosity decrease when the pectin chains contain less carboxyl group (more hydrophobic). This result suggests that the Ca^{2+} bridge, through the interaction with carboxyl group in pectin chains, dominates the rheological properties of pectin gels in the presence of Ca^{2+}, as described in the egg-box model.[31,32] Furthermore, From P1 to P2, the increase of methoxyl content leads to the compact junctions due to hydrophobic interaction in the gel network, resulting in the yield point appearing in a lower frequency region (long time scale). From P1 to P3, the increase of amide group leads to a decrease of G', which may be due to the stronger ability of the amide group to form hydrogen bonding with water than with pectin chains.[59]

Figure 7b shows the effects of calcium ion concentration $[Ca^{2+}]$ on the rheological properties in P1 solutions. The variation of $[Ca^{2+}]$ directly changes the ratio $R = 2[Ca^{2+}]/[COO^-]$, which is a key parameter to control the sol−gel transition in low methoxyl pectin aqueous solutions.[60,61] It can be seen that, in the absence of Ca^{2+}, both G' and G'' have a small value (about several pascals) within the whole frequency range studied. In the low-frequency range (<20 rad/s), G' is slightly larger than G'', while at the higher frequency (>20 rad/s), G' becomes slightly larger than G', suggesting that the system is a viscoelastic solution. The increase of $[Ca^{2+}]$ translates the pectin solution from sol to gel, but the G' of pectin gel in the high-frequency region levels off when $[Ca^{2+}]$ is high enough, suggesting the formation of a gel-like structure. The scaling exponent in the high-frequency region Δ decreases as $[Ca^{2+}]$ increases because more Ca^{2+} ions result in the formation of denser junctions in a gel network, as evidenced by the nearly frequency-independent storage modulus.

Figure 7c shows the effects of pectin concentration on the rheological properties of P1 aqueous solutions. It can be seen that both G' and viscosity significantly increase as the pectin concentration increases. For the scaling exponent, since the pectin solution is more homogeneous in 0.5% P1 solution than in 2% P1 solution, the scaling exponent of frequency dependence in 0.5% P1 solution is slightly smaller than that in 2% P1 solution.

Discussion

In order to correlate the results of rheological measurements with Monte Carlo simulation, the frequency-dependent power exponents in the high-frequency region, the solution status (sol or gel) determined by tilting tube methods,[62,63] the ratio R, and the composition of the pectin solutions are summarized in Table 3. When R increases, the ability to form gel is enhanced, and the scaling exponents decrease because the modulus of the gel network is strengthened. If we correlate the ratio R of pectin aqueous solutions in rheological measurements with the polar group saturation k_{sa} in Monte Carlo simulation, a qualitatively consistent conclusion can be made: that is, increasing the polar group saturation of amphiphilic polymer chains in solution can greatly promote physical gelation and strengthen the gel network.

Conclusion

In this paper, we have used Monte Carlo simulation to study the effects of polar group saturation on the physical gelation in amphiphilic polymer solutions, and the simulation results have

TABLE 3: Results of Rheological Experiments from Various Pectin Solutions[a]

composition	P1 (2%), no Ca^{2+}	P1 (2%), 5 mM Ca^{2+}	P2 (2%), 5 mM Ca^{2+}	P3 (2%), 5 mM Ca^{2+}	P1 (2%), 10 mM Ca^{2+}	P1 (0.5%), 5 mM Ca^{2+}
R	0	0.066	0.088	0.092	0.132	0.265
status	sol	sol/gel	sol	gel	gel	gel
Δ	0.35	0.23	0.35	0.16	0.11	0.08

[a] Status is the sol/gel state determined by the tilting tube method.[57,58] R, which equals $2[Ca^{2+}]/[COO^-]$, is used to record the saturation of carboxyl groups in pectin chains. Δ is the scaling exponent of the storage modulus at high shear frequency region (ω > 20 rad/s).

been compared with the rheological experiments on pectin aqueous solutions. We have also investigated the effects of different solvent conditions to the backbone and side chain of the comblike coarse grained amphiphilic polymer chain on polymer chain conformation, and different gelation mechanisms have been discussed. Both the simulation and experimental results reveal that the increase of the polar group saturation can significantly promote physical gelation and strengthen the gel network.

Acknowledgment. We thank Dr. Jozef Kokini for the use of ARES rheometer. This work was supported by ACS−PRF (41333-G7) (Q.R.H) and the National Natural Science Foundation of China (20674086, 20620120105, 50503022) and the Fund for Creative Research Groups (50621302) (L.J.A. and T.F.S.) and subsidized by the Special Funds for Major State Basic Research Projects (No. 2005CB623800).

Supporting Information Available: Graph of simulation time dependence of the root-mean-square radius of gyration and the diffusion coefficient and snapshots of the single chain conformation. This material is available free of charge via the Internet at http://pubs.acs.org.

References and Notes

(1) Jain, S.; Bates, F. S. *Science* **2003**, *300*, 460.
(2) Alexandridis, P.; Olsson, U.; Lindman, B. *Langmuir* **1998**, *14*, 2627.
(3) Yamamoto, S.; Maruyama, Y.; Hyodo, S. *J. Chem. Phys.* **2002**, *116*, 5842.
(4) Hoefler, A. C. Ph.D. Thesis, University of Delaware, 2003.
(5) Valstar, A. Ph.D. Thesis, Uppsala University, 2000.
(6) Guillotin, S. Ph.D. Thesis, Wageningen University, 2005.
(7) Gittings, M. R.; Cipelletti, L.; Trappe, V.; Weitz, D. A.; In, M.; Lal, J. *J. Phys. Chem. A* **2001**, *105*, 9310.
(8) Jiang, J.; Sandler, S. I. *Langmuir* **2006**, *22*, 5702.
(9) Stevens, M. J. *J. Chem. Phys.* **2004**, *121*, 11942.
(10) Tepper, H. L.; Voth, G. A. *J. Chem. Phys.* **2005**, *122*, 124906.
(11) Chen, C.-M.; Fwu, Y.-A. *Phys. Rev. E* **2000**, *63*, 011506.
(12) Bates, M. A. *J. Chem. Phys.* **2004**, *120*, 2026.
(13) Girardi, M.; Henriques, V. B.; Figueiredo, W. *Chem. Phys.* **2006**, *328*, 139.
(14) Arya, G.; Panagiotopoulos, A. Z. *Phys. Rev. E* **2004**, *70*, 031501.
(15) Vasilevskaya, V. V.; Khalatur, P. G.; Khokhlov, A. R. *Macromolecules* **2003**, *36*, 10103.
(16) Firetto, V.; Floriano, M. A.; Panagiotopoulos, A. Z. *Langmuir* **2006**, *22*, 6514.
(17) Skepo, M.; Linse, P.; Arnebrant, T. *J. Phys. Chem. B* **2006**, *110*, 12141.
(18) Paul, W.; Binder, K.; Kremer, K.; Heermann, D. W. *Macromolecules* **1991**, *24*, 6332.
(19) Tries, V.; Paul, W.; Baschnagel, J.; Binder, K. *J. Chem. Phys.* **1997**, *106*, 138.
(20) Lau, K. F.; Dill, K. A. *Macromolecules* **1989**, *22*, 3986.
(21) Lau, K. F.; Dill, K. A. *Proc. Natl. Acad. Sci. U.S.A.* **1990**, *87*, 6388.
(22) Oberdorf, R.; Ferguson, A.; Jacobsen, J. L.; Kondev, J. *Phys. Rev. E* **2006**, *74*, 051801.
(23) Schnabel, S.; Bachmann, M.; Janke, W. *Phys. Rev. Lett.* **2007**, *98*, 048103.
(24) Larson, R. G. *J. Chem. Phys.* **1988**, *89*, 1642.
(25) Glotzer, S. C.; Paul, W. *Annu. Rev. Mater. Res.* **2002**, *32*, 401.
(26) Paul, W. *Multiscale Computational Methods in Chemistry and Physics*; Brandt, A., Bernholc, J., Binder, K., Eds.; IOS Press: Amsterdam, 2001; p 285.
(27) Freire, J. J. *Adv. Polym. Sci.* **1999**, *143*, 35.
(28) Loison, C. Ph.D. Thesis, Max Planck Institute, 2003.
(29) Kortemme, T.; Morozov, A. V.; Baker, D. *J. Mol. Biol.* **2003**, *326*, 1239.
(30) Goycoolea, F. M.; Cardenas, A. *J. PACD* **2003**, 17.
(31) Morris, E. R.; Powell, D. A.; Gidley, M. J.; Rees, D. A. *J. Mol. Biol.* **1982**, *155*, 507.
(32) de Kerchove, A. J.; Elimelech, M. *Macromolecules* **2006**, *39*, 6558.
(33) Li, Y. Q.; Huang, Q. R.; Shi, T. F.; An, L. J. *J. Phys. Chem. B* **2006**, *110*, 23502.
(34) Deutsch, H. P.; Binder, K. *J. Chem. Phys.* **1991**, *94*, 2294.
(35) Carmesin, I.; Kremer, K. *Macromolecules* **1988**, *21*, 2819.
(36) Yannick, R. *Macromol. Theory Simul.* **1998**, *7*, 359.
(37) Vasilevskaya, V. V.; Klochkov, A. A.; Khalatur, P. G.; Khokhlov, A. R.; ten Brinke, G. *Macromol. Theory Simul.* **2001**, *10*, 389.
(38) Jiang, Y.; Perahia, D.; Wang, Y.; Bunz, U. H. F. *Macromolecules* **2006**, *39*, 4941.
(39) Peng, D.; Zhang, X.; Huang, X. *Macromolecules* **2006**, *39*, 4945.
(40) Wilding, N. B.; Müller, M.; Binder, K. *J. Chem. Phys.* **1996**, *105*, 802.
(41) Carmesin, I.; Kremer, K. *Macromolecules* **1988**, *21*, 2819.
(42) Yang, Y.; Lu, J.; Yang, D.; Ding, J. *Macromol. Theory Simul.* **1994**, *3*, 731.
(43) Metropolis, N.; Rosenbluth, A. W.; Rosenbluth, M. N.; Teller, A. H. *J. Chem. Phys.* **1953**, *21*, 1087.
(44) Picout, D. R.; Richardson, R. K.; Morris, E. R. *Carbohydr. Polym.* **2000**, *43*, 123.
(45) Li, Y. Q.; Sun, Z. Y.; Shi, T. F.; An, L. J. *J. Chem. Phys.* **2004**, *121*, 1133.
(46) Lootens, D.; Capel, F.; Durand, D.; Nicolai, T.; Boulenguer, P.; Langendorff, V. *Food Hydrocolloids* **2003**, *17*, 237.
(47) Matia-Merino, L.; Lau, K.; Dickinson, E. *Food Hydrocolloids* **2004**, *18*, 271.
(48) Liu, Y.; Pandey, R. B. *J. Chem. Phys.* **1996**, *105*, 825.
(49) Liu, Y.; Pandey, R. B. *Phys. Rev. E* **1996**, *54*, 6609.
(50) Li, Y. Q.; Sun, Z. Y.; Su, Z. H.; Shi, T. F.; An, L. J. *J. Chem. Phys.* **2005**, *122*, 194909.
(51) Ganazzoli, F.; Raos, G.; Allegra, G. *Macromol. Theory Simul.* **1999**, *8*, 65.
(52) Philipse, A. P.; Wierenga, A. M. *Langmuir* **1998**, *14*, 49.
(53) Meller, A.; Gisler, T.; Weitz, D. A. *Langmuir* **1999**, *15*, 1918.
(54) Anderson, J. A.; Travesset, A. *Macromolecules* **2006**, *39*, 5143.
(55) Holst, P. S.; Kjøniksen, A.-L.; Bu, H.; Sande, S. A.; Nyström, B. *Polym. Bull.* **2006**, *56*, 239.
(56) Bromberg, L. *Macromolecules* **1998**, *31*, 6148.
(57) Nitta, Y.; Kim, B. S.; Nishinari, K.; Shirakawa, M.; Yamatoya, K.; Oomoto, T.; Asai, I. *Biomacromolecules* **2003**, *4*, 1654.
(58) Bhatia, S. R.; Mourchid, A. *Langmuir* **2002**, *18*, 6469.
(59) Thakur, B. R.; Singh, R. K.; Handa, A. K. *Crit. Rev. Food Sci. Nutr.* **1997**, *37*, 47.
(60) Fu, J.-T.; Rao, M. A. *Food Hydrocolloids* **1999**, *13*, 371.
(61) Fu, J.-T.; Rao, M. A. *Food Hydrocolloids* **2001**, *15*, 93.
(62) Werner, B.; Bu, H.; Kjøniksen, A.-L.; Sande, S. A.; Nyström, B. *Polym. Bull.* **2006**, *56*, 579.
(63) Wellinghoff, S.; Shaw, J.; Baer, E. *Macromolecules* **1979**, *12*, 932.